Spontaneous direct band-gap, high hole mobility and huge exciton energy in atomic-thin TiO_2 nanosheet

Wei Zhou[1,2], Naoto Umezawa[2], Renzhi Ma[2], Nobuyuki Sakai[2], Yasuo Ebina[2], Koki Sano[3,4], Mingjie Liu[4], Yasuhiro Ishida[4], Takuzo Aida[3,4], and Takayoshi Sasaki[2*]*

1. Department of Applied Physics, Tianjin Key Laboratory of Low Dimensional Materials Physics and Preparing Technology, School of Science, Tianjin University, Tianjin 300072, P. R. China.

2. International Center for Materials Nanoarchitectonics (WPI-MANA), National Institute for Materials Science, 1-1, Namiki, Tsukuba, Ibaraki 305-0044, Japan.

3. Department of Chemistry and Biotechnology, School of Engineering, The University of Tokyo, 7-3-1 Hongo, Bunkyo-ku, Tokyo 113-8656, Japan.

4. RIKEN Center for Emergent Matter Science, 2-1 Hirosawa, Wako, Saitama 351-0198, Japan.

*E-mail: weizhou@tju.edu.cn; SASAKI.Takayoshi@nims.go.jp

Section 1:

1.1 Convergence test for G_0W_0 calculations

To perform the convergence test for the G_0W_0 calculations, the QP band gap of LNS-TiO_2 nanosheet related with the *k* points mesh and number of bands was calculated and present in Figure S1. The results indicate the parameters used in our work (k-mesh of 17×15×1 and band number of 240) give a quite good convergence for the QP band gap.

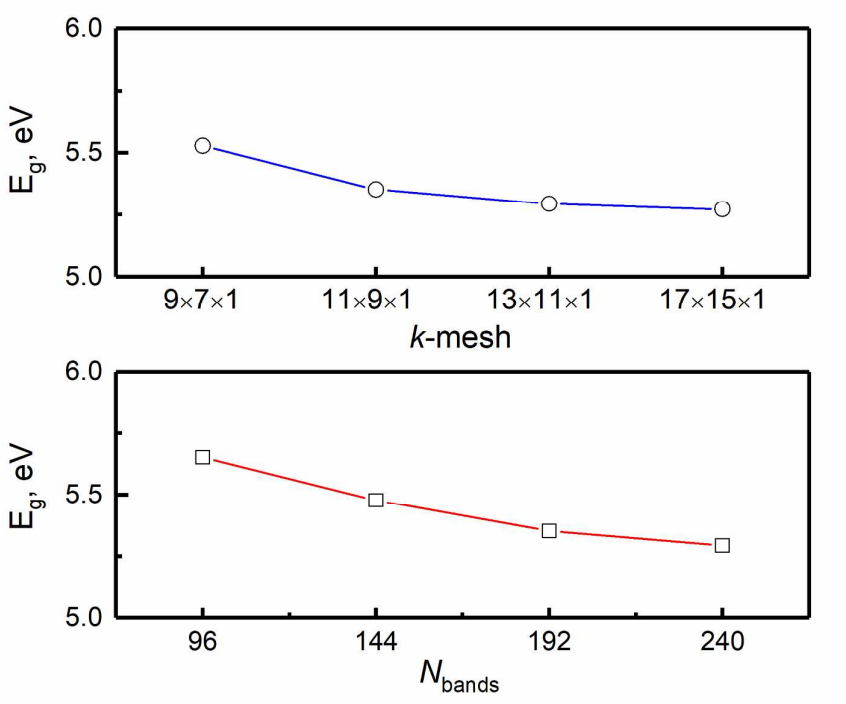

Figure S1. The QP band gap related with (a) *k* points mesh and (b) number of bands from G_0W_0 calculations.

1.2 Bonding analysis

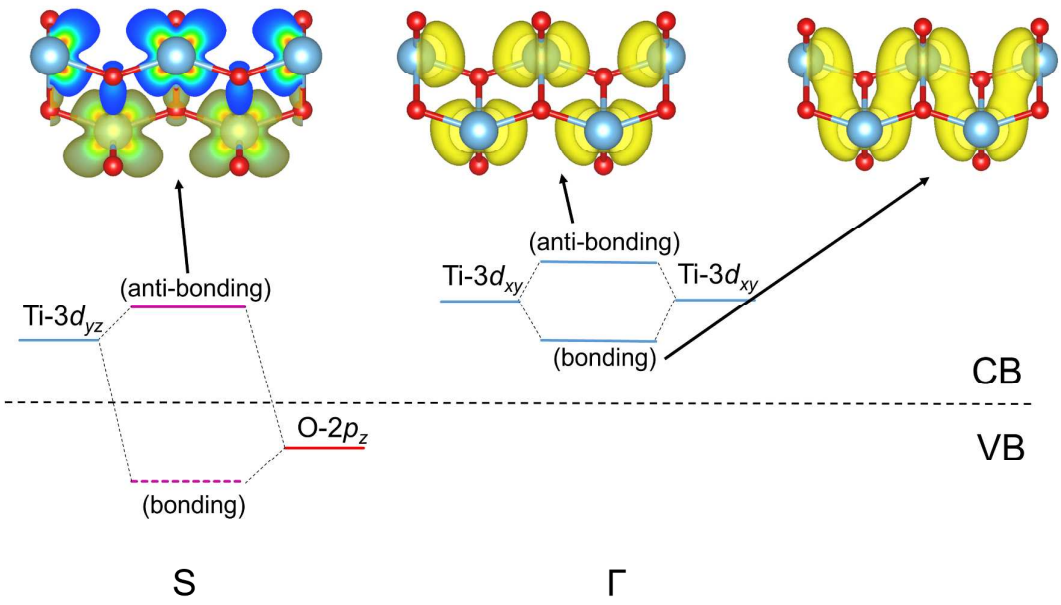

Figure S2. Partial charge density isosurfaces (0.002 e/Å^3) for the hybridization states at specific high symmetry *k* points (S and Γ points) of CB in LNS-TiO_2, and the orbital bonding schematic diagram is predicted based on the bonding character analysis.

1.3 Flatband for exciton in LNS-TiO_2

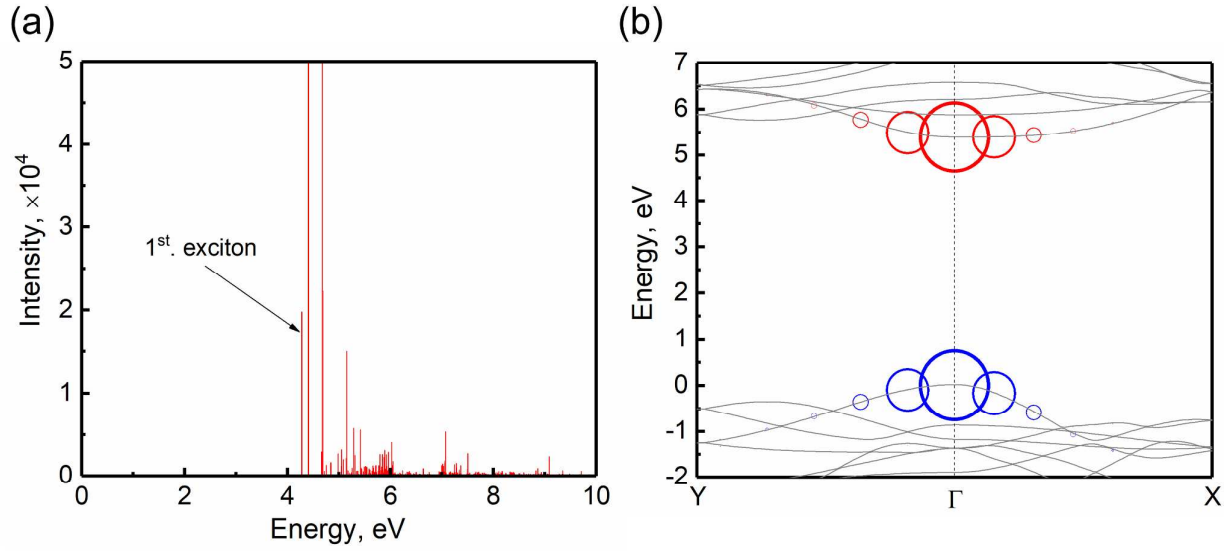

Figure S3. (a) The oscillator strength of exciton for LNS-TiO_2, and (b) the electron-hole pairs contributions for the first BSE eigenstate (radius of circle indicates the absolute value of coupling coefficient).

Section 2:

Experimental test for optical absorption of LNS-TiO_2 nanosheets

A superconducting magnet JASTEC model JMTD-10T100 with a bore of 100 mm was used for magnetic orientation of titanate nanosheets. Polarized electronic absorption spectra were recorded on a JASCO model V-570 UV/VIS spectrophotometer. An aqueous dispersion of titanate nanosheet was prepared according to literature[S1] and deionized by repeated centrifugation and re-dispersion with water.[S2] Poly (vinyl alcohol) (degree of polymerization = 1750 ± 50) was purchased from Tokyo Chemical Industry (TCI) and used as received.

An aqueous dispersion (3.0 mL) of titanate nanosheet (5×10^{-4} wt%) containing poly(vinyl alcohol) (7.0 wt%) was charged into a quartz optical cell (10 mm × 10 mm). The cell was then placed in the bore of a superconducting magnet (10 T) in such a way that the light path of the cell was directed parallel (sample A) or perpendicular (sample B) to the applied magnetic field and allowed to stand at 20 °C for 20 minutes. Titanate nanosheets are known to align perpendicular to the applied magnetic field.[S3]

Then, the sample was transferred to an electronic absorption spectrometer equipped with a polarizer for obtaining its polarized absorption spectrum at 20 °C. Despite the absence of magnetic field during the absorption measurement, relaxation of the alignment of titanate nanosheet was slow and negligible, owing to the effect of poly (vinyl alcohol) as a thickener. In the case of sample A, the absorption spectrum was essentially independent of the polarization direction of the incident light. In the case of sample B, the incident light was polarized perpendicular to the direction of the magnetic field that was applied before the absorption measurement. The in-plane average optical absorption was obtained from the average of absorption measurement with the polarization direction of incident light along the in-plane directions of tianate nanosheet (Figure 7, left inset).

Section 3:

Calculations for defects (oxygen vacancy or titanium vacancy) in LNS-TiO_2 nanosheet

To consider the influence of defects, the LNS-TiO_2 nanosheet model (54 atoms supercell) with one oxygen vacancy (O_V) or titanium vacancy (Ti_V) was simulated. Here, hybrid functional calculations were performed since the quasi-particle calculations for supercell model with large size is difficult and quite time consuming. As depicted in Figure S4(a), new impurity states form in the band gap to reduce the optical transition energy. This is also confirmed by the optical absorption spectrum of Figure S4(b) that significant defect-related absorption will appear at the low energy region (less than 3 eV), while the intrinsic optical band edge at high energy region is nearly unchanged. In our experimental absorption spectrum (Figure 7 in the manuscript), no observable defect-related absorption peak can be found at the low energy region. Thus, it is thought that the influence of defects on the optical absorption can be negligible in this work.

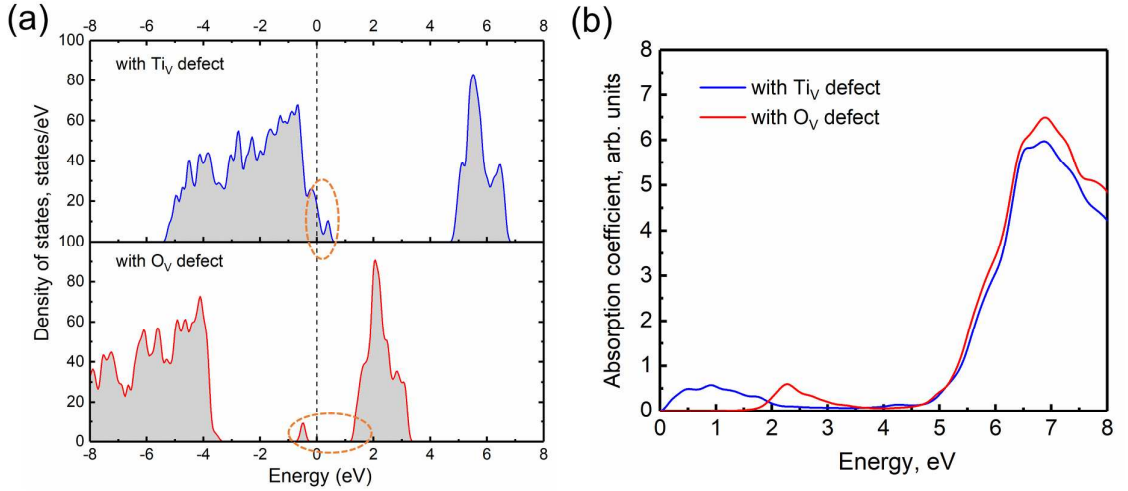

Figure S4. The calculated density of states for LNS-TiO_2 nanosheet with Ti_V or O_V defect (dashed black line indicates the Fermi level), (b) the calculated absorption coefficient of LNS-TiO_2 nanosheet with Ti_V or O_V defect.

Section 4:

Experimental test for hydrogen production of LNS-TiO_2 nanosheets

LNS-TiO_2 nanosheets were flocculated with KCl solution and the resulting restacked sample was employed as a photocatalyst. H_2O 300 ml + CH_3OH 30 ml was introduced into A Pyrex reaction vessel and 0.1 g of the restacked sample was dispersed under magnetic stirring. Then Ar at a pressure of 112 Torr was circulated in the reaction cell while irradiated by 500 W Xe lamp from outside. Evolved H_2 gas was determined by gas chromatography. The test results are shown in Figure S5 below. And the average H_2 production rate is estimated to 7.6 μmol/h.

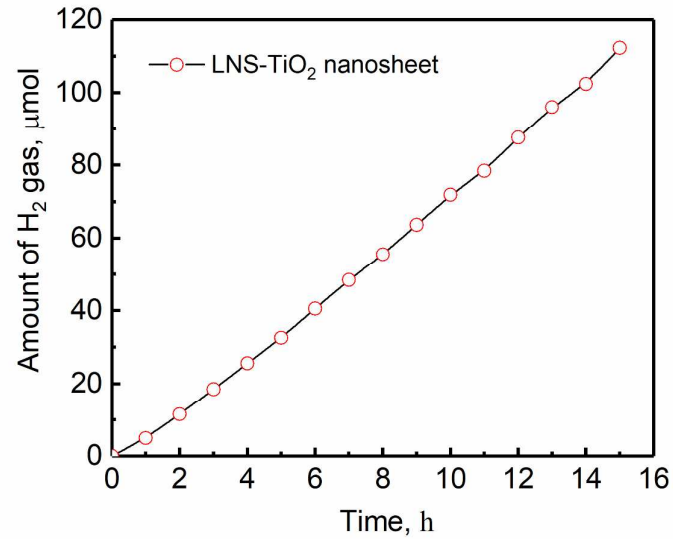

Figure S5. The experimental results for H_2 production of LNS-TiO_2 nanosheet.

Reference:

S1. Tanaka, T.; Ebina, Y.; Takada, K.; Kurashima, K.; Sasaki, T., Oversized Titania Nanosheet Crystallites Derived from Flux-Grown Layered Titanate Single Crystals, *Chem. Mater.* **2003**, *15*, 3564–3568.

S2. Sano, K.; Kim, Y. S.; Ishida, Y.; Ebina, Y.; Sasaki, T.; Hikima, T.; Aida, T., Photonic Water Dynamically Responsive to External Stimuli, *Nat. Commun.* **2016**, *7*, 12559.

S3. Liu, M.; Ishida, Y.; Ebina, Y.; Sasaki, T.; Hikima, T.; Takata, M.; Aida, T., An Anisotropic Hydrogel with Electrostatic Repulsion between Cofacially Aligned Nanosheets, *Nature* **2015**, 517, 68–72.